Available online at www.sciencedirect.com
SCIENCE DIRECT®
International Journal of Heat and Mass Transfer 47 (2004) 2149–2159
International Journal of HEAT and MASS TRANSFER
www.elsevier.com/locate/ijhmt

Bubble nucleation in response to a step change in heat flux

Ross L. Judd *, Andrej Simjanov

Department of Mechanical Engineering, McMaster University, Hamilton, Ont., Canada L8S 4L7

Received 30 July 2003; received in revised form 1 December 2003

Abstract

An experimental investigation of dichloromethane boiling on a transparent glass heater surface is reported in which the appearance of bubbles in response to a step change in heat flux at various levels of system pressure was observed and recorded by means of a high-speed video camera. The results of the investigation established that Classical nucleation theory is not valid and that the Hsu and Han & Griffith nucleation models, which are based upon it, are unable to predict the conditions under which nucleation will occur. However, the Madejski nucleation theory, proposed over 40 years ago but never tested experimentally, appears to be able to reliably predict the conditions under which a bubble will appear on a surface undergoing nucleate pool boiling.

1. Introduction to nucleate boiling

The aspect of boiling that has attracted the attention of many equipment designers is the high rate of heat transfer associated with the phenomenon so that it has found application in many industries where heat has to be removed efficiently in confined spaces, such as nuclear reactors, steam generators, turbines, rockets and commercial evaporators. A closer look at nucleate boiling reveals that the bubbles always form at the same locations on the heater surface known as nucleation sites, which have been identified as imperfections in the surface such as tiny pits, cracks or scratches. Microscopic investigation has revealed that these imperfections are naturally occurring on all surfaces, but only those that can trap a vapour residue when the liquid contacts the surface become active as nucleation sites [1,2].

After a bubble has left the heater surface, the nucleation site becomes inactive for a period of time known as the waiting time t_w, even though a nucleus remains at the cavity from which the bubble departed. In order for the nucleus to commence growing into a bubble once again, it must be surrounded by liquid warmer than the vapour within it, which provides the heat that causes evaporation of the liquid at the vapour–liquid interface. After the liquid contacts the heater surface, energy diffuses into it and the thickness of the superheated layer δ increases until the thickness has grown sufficiently to encompass the nucleus, thereby enabling it to grow.

As it continues to draw heat from the superheated liquid layer, the nucleus develops into a bubble during the growth time t_g until it reaches departure size R_b. If, however, a bubble grows larger than the superheated layer thickness δ into the relatively colder bulk liquid at temperature T_∞, it loses heat and collapses on the heater surface. Whether it departs or collapses, bulk liquid at temperature T_∞ replaces it and the cycle repeats. Assuming each bubble to be responsible for the removal of the same amount of heat, it was originally believed that the total heat transferred by nucleate boiling could be predicted if the number of nucleation sites on a given heater surface N/A were known and the frequency of bubble emission f could be determined in accordance with $1/f = t_w + t_g$. While this is no longer felt to be correct, it follows that the temperature distribution in the liquid surrounding the nucleation site and the conditions that have to be satisfied for a bubble to commence growing have to be known.

Different nucleation criteria have been postulated and various nucleation heat transfer models have been advanced over the years [3–6]. However, due to the

* Corresponding author. Tel.: +1-905-525-9140; fax: +1-905-572-7944.
E-mail address: juddr@mcmaster.ca (R.L. Judd).

0017-9310/$ - see front matter © 2004 Elsevier Ltd. All rights reserved.
doi:10.1016/j.ijheatmasstransfer.2003.12.007

Nomenclature

A	nucleation parameter $A = 2\sigma T_{sat}/\rho_v h_{fg}$, m °C
b	bubble nucleus height, m
C	specific heat, kJ/kg °C
f	bubble emission frequency, 1/s
g	gravitational acceleration, m/s^2
h_{fg}	latent heat, kJ/kg
Ja	Jakob number $Ja = \rho_l C_l \theta_{sup}/\rho_v h_{fg}$
p	pressure, kN/m^2
p_l	liquid pressure, kN/m^2
p_v	vapour pressure, kN/m^2
p_∞	ambient pressure, kN/m^2
q''	heat flux, kW/m^2
q''_l	heat flux to liquid, kW/m^2
q''_s	heat flux to surface, kW/m^2
r	radius, m
R	bubble radius, m
R_b	bubble departure radius, m
R_c	nucleation cavity radius, s
t	time, s
t_g	bubble growth time, s
t_w	bubble waiting time, s
T	temperature, °C
T_{sat}	saturation temperature, °C
T_v	vapour temperature, °C
T_∞	ambient temperature, °C
y	displacement from surface, m

Greek symbols

α	thermal diffusivity, m^2/s
β	contact angle, °
δ	thermal layer thickness, m
θ	temperature difference, °C
ρ	density, kg/m^3
σ	surface tension, N/m
τ	time period, s

complexity of the boiling phenomenon, these models have had limited success. The fact that the time intervals involved are extremely short and that the events take place on a microscopic scale, imposes great technical difficulty with regard to validating these models. This investigation is an attempt to explore the validity of the nucleation criteria and to gain further insight into the nucleation process. Experimental data were obtained on a transparent stannic oxide coated glass heater surface. The response to a step change of heat flux was investigated for a number of different naturally occurring nucleation sites at various levels of system pressure and heat flux. Bubbles nucleating on the upper surface of the heater were observed from underneath and the data gathered was used to investigate the predictions of the nucleation criteria.

2. Classical nucleation theory

Bubbles in nucleate boiling play a double role. During their growth, especially when buoyancy forces lift them from the heating surface, they create significant agitation in the surrounding liquid. Since natural convection still occurs around the nucleation sites, this agitation markedly increases the transfer of heat. At the same time, liquid evaporation at the bubble–liquid interface removes the heat that is supplied at the heating surface. In this way bubbles move heat into the bulk liquid, which results in higher heat transfer coefficients. The necessity of understanding the nucleation phenomenon is therefore obvious if nucleate boiling is to be enhanced and the performance of a heating surface is to be optimised.

It has been observed experimentally that in order for bubbles to form at a heater surface, a phenomenon known as heterogeneous boiling, the temperature of the heater surface T_w must exceed the liquid saturation temperature T_{sat} sufficiently. Bubbles can nucleate in the bulk of a liquid as well, a phenomenon known as homogenous boiling, but in order for this to happen, the superheat $\theta_w = T_w - T_{sat}$ has to be an order of magnitude greater than that required for heterogeneous boiling.

For a bubble of radius r to exist in a uniformly superheated liquid, the forces resulting from the difference between the pressure inside the bubble p_v and the pressure in the liquid p_l acting on its projected area πr^2 and the surface tension σ acting on its circumference $2\pi r$ must be balanced in accordance with the relationship below.

$$p_v - p_l = \frac{2\pi r\sigma}{\pi r^2} = \frac{2\sigma}{r} \tag{1}$$

In the bulk of a pure and degassed liquid of infinite extent, embryos with very small radii exist that could serve as nuclei, but it can be seen from Eq. (1) that a high pressure difference force $\pi r^2(p_v - p_l)$ would be needed to overcome the surface tension force $2\pi r\sigma$. Hence, highly superheated liquid would be required in the vicinity of the vapour nucleus. In most engineering applications, however, the surface contains cavities in which vapour can be trapped. For a combination of relatively large contact angles, which accompany poorly

wetting liquids, and relatively small cavity radius to depth ratio, advancing liquid may reach the opposite wall of the cavity before displacing the vapour completely. Thus a nucleus with cavity radius R_c is formed which enables boiling to take place on the heater surface when the liquid around the nucleus is sufficiently superheated.

If the temperature inside the bubble T_v evaluated at p_v is higher than the temperature of the surrounding liquid T_l evaluated at p_l, heat will flow outward, the vapour will condense at the liquid/vapour interface and the bubble will collapse. If, however, the liquid is brought to a temperature T_l higher than the vapour temperature T_v in the bubble, heat will flow inward, the liquid will evaporate at the liquid/vapour interface, the bubble will grow and eventually depart from or collapse at the heater surface. Since evaporation is a reversible, isothermal and isobaric process, the Clausius–Clapeyron equation $dp/dT = \rho_v h_{fg}/T_{sat}$ may be employed, leading to the relationship

$$p_v - p_l = \frac{\rho_v h_{fg}(T_v - T_{sat})}{T_{sat}} = \frac{2\sigma}{R_c} \tag{2}$$

The superheat required for a nucleus having radius R_c to commence growing into a bubble is

$$T_v - T_{sat} = \frac{2\sigma T_{sat}}{\rho_v h_{fg} R_c} = \frac{A}{R_c} \tag{3}$$

where the nucleation parameter A is given by $A = 2\sigma\, dT/dp = 2\sigma T_{sat}/\rho_v h_{fg}$. This analysis demonstrates that a nucleus having radius R_c can grow into a bubble in a uniformly superheated liquid if it is surrounded by warmer liquid such that $\theta_v = T_v - T_{sat} = \theta_\infty = A/R_c$.

However, in nucleate boiling, a temperature gradient is always present at the heater surface. Nevertheless, it has been argued that a nucleus can still develop into a bubble if the temperature of the liquid surrounding the nucleus is equal to or greater than the temperature of the vapour inside the bubble. Fig. 1 schematically depicts the development of the dimensionless temperature profiles θ/θ_∞ in a liquid adjacent to a surface having superheat θ_w as a function of dimensionless distance $\delta/R_c = \sqrt{\pi\alpha_l t_w}/R_c$ where R_c is the radius of the hemispherical vapour nucleus. As time t increases, the straight lines representing the asymptotes to the temperature profiles rotate counter-clockwise until at the end of the waiting period at which time $t = t_w$, the temperature profile passes through the point at which $\theta_v/\theta_\infty = 1$ and $b/R_c = 1$. At this moment in time, the conditions required for the nucleation of a hemispherical vapour nucleus are satisfied in as much as all the way from the surface to the tip, the vapour nucleus is surrounded by liquid having superheat equal to or greater than θ_v.

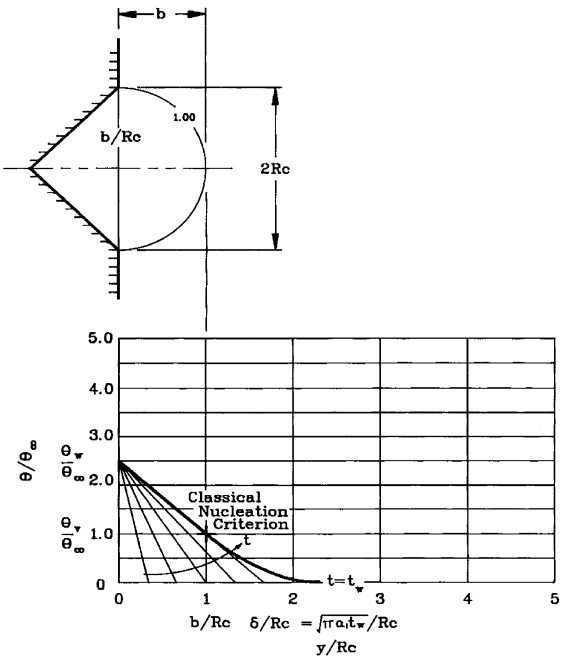

Fig. 1. Schematic representation of the Classical nucleation theory.

The equation of the straight line passing through the point at which $\theta_v/\theta_\infty = 1$ and $b/R_c = 1$ which represents the Classical nucleation criterion is expressed by the relationship

$$\frac{\theta}{\theta_\infty} = \frac{\theta_w}{\theta_\infty}\left[1 - \frac{y/R_c}{\sqrt{\pi\alpha_l t_w}/R_c}\right] \tag{4}$$

Substituting the coordinates of the point representing the Classical nucleation theory into this equation reveals that a bubble will commence growing whenever the relationship

$$\frac{\theta_\infty}{\theta_w} = \frac{A/R_c}{\theta_w} = \left[1 - \frac{R_c}{\sqrt{\pi\alpha_l t_w}}\right] \tag{5}$$

is satisfied. This concept is the basis of the Hsu model [3] and the Han and Griffith model [4].

2.1. Hsu model

Hsu [3] postulated that when a bubble departs from a nucleation site, the superheated thermal layer surrounding it is destroyed and relatively cold liquid from the bulk rushes in to fill the void. During the time required for the newly arrived liquid to warm up sufficiently to enable bubble growth to commence, heat diffuses into the liquid and the thickness of the superheated layer increases, although its thickness is limited, due to the strong turbulence in the bulk liquid. When the temperature of the superheated liquid at the site exceeds

the vapour temperature, the bubble starts to grow. When a bubble reaches departure size, it moves away from the site, leaving a vapour residue in the nucleation cavity from which the next bubble will be formed.

Assuming the wall superheat θ_w to be constant, Hsu solved the unsteady diffusion equation to determine the temperature profile in the liquid $\theta(y,t)$ subject to the initial and boundary conditions $\theta(y,0)=0$, $\theta(0,t)=\theta_w$ and $\theta(\delta,t)=0$. The waiting time was deemed to have ended when the temperature profile passed through the point (θ_v, b) corresponding to the tip of the nucleus where $\theta_v=\theta_\infty$, thereby satisfying the Classical nucleation criterion. The value of waiting time so determined combined with the value of growth time predicted by a relationship for bubble growth from inception to departure enabled the bubble period and the frequency of bubble emission to be determined. However, it has been reported by Shoukri and Judd [5] that this model does not represent the nucleation phenomenon very well. Nevertheless, the Hsu model has provided the foundation and motivation for a number of researchers and is an important milestone in the development of the nucleate boiling theory.

2.2. Han and Griffith model

Han and Griffith [4] also assumed a growing bubble to be surrounded by a superheated liquid layer. They observed through high-speed photography that although the bubble radius may extend beyond the thickness of the superheated layer, the very fast growth in the first few moments pushes the thermal layer ahead of it so that the bubble is enveloped by superheated fluid from inception until departure. When the bubble departs, the liquid that fills the void is assumed to be heated by transient conduction.

Assuming constant wall temperature T_w, Han and Griffith obtained the temperature profile in the liquid $T(y,t)$ by solving the unsteady diffusion equation subject to the initial and boundary conditions $T(y,0)=T_\infty$, $T(0,t)=T_w$, $T(\infty,t)=T_\infty$. The temperature distribution obtained was approximated by a straight line with a slope of $(T_w-T_\infty)/\delta(t)$ where $\delta(t)=\sqrt{\pi\alpha_l t}$ is the thickness of the thermal layer. The time required for the thickness of the thermal layer to increase to $\delta(t_w)=\sqrt{\pi\alpha_l t_w}$ is the waiting time t_w. When the temperature at distance $3/2R_c$ from the heater surface was equivalent to the temperature of the vapour in the nucleus $T_v=T_{sat}+A/R_c$, the waiting time was deemed to have ended, thereby satisfying the Classical nucleation criterion. Similar to the previous model, the value of waiting time so determined combined with the value of growth time predicted by a relationship for bubble growth from inception to departure enabled the bubble period and the frequency of bubble emission to be determined.

At the time when Han and Griffith's model was advanced, it was believed that the physics behind the nucleation process, bubble growth and departure was completely understood. However, the researchers were not able to measure the cavity sizes in question and therefore had to use hypothetical values to interpret their results. It was thought that the relatively poor agreement between the model predictions and the experimental data was due to this fact.

3. Madejski nucleation theory

Madejski [7] argued that a vapour nucleus is hemispherical only if it exists in a uniform temperature field. If there is a temperature gradient in the liquid surrounding the vapour nucleus, its shape will be spheroidal and it will require greater superheat than that required by a hemispherical nucleus for nucleation to occur.

For simplicity in the analysis, the linear temperature profile below was used to represent the temperature distribution in the liquid adjacent to the heater surface.

$$\frac{T(y)-T_{sat}}{T_w-T_{sat}}=1-\frac{y}{\delta} \tag{6}$$

The geometry of the spheroid and the principal radii associated with it are given by

$$y=b\left(1-\frac{r^2}{R_c^2}\right),\quad R_1=-\frac{1}{y''}(1+y'^2)^{3/2},$$
$$R_2=-\frac{r}{y'}(1+y'^2)^{1/2} \tag{7}$$

where y' and y'' are the first and second derivatives of y with respect to r. Combination of these relationships leads to the equation governing the profile of the vapour nucleus

$$\frac{1}{R_1}+\frac{1}{R_2}=-\frac{1}{r}\left[\frac{\mathrm{d}}{\mathrm{d}r}\left(\frac{ry'}{\sqrt{1+y'^2}}\right)\right] \tag{8}$$

The modified Laplace–Kelvin equation for a non-spherical interface can be written as

$$\frac{\rho_l-\rho_v}{\rho_l}(p_\infty-p_l)=\sigma\left(\frac{1}{R_1}+\frac{1}{R_2}\right) \tag{9}$$

Eq. (9) combined with the Clausius–Clapeyron equation leads to the relationships

$$\theta(y)=T(y)-T_{sat}=(p_\infty-p_l)\frac{T_{sat}}{\rho_v h_{fg}}$$
$$=\frac{\rho_l}{\rho_l-\rho_v}\sigma\left(\frac{1}{R_1}+\frac{1}{R_2}\right)\frac{T_{sat}}{\rho_v h_{fg}} \tag{10}$$

$$\theta(y)=\frac{\rho_l}{\rho_l-\rho_v}\frac{A}{2}\left(\frac{1}{R_1}+\frac{1}{R_2}\right) \tag{11}$$

where $A = 2\sigma T_{sat}/\rho_v h_{fg}$. For the uniform superheat case in which $R_1 = R_2 = R_c$, then

$$\frac{1}{R_1} + \frac{1}{R_2} = \frac{2}{R_c} \tag{12}$$

and $\theta(y)$ is invariant and equal to θ_∞. Under these conditions, Eq. (11) becomes

$$\theta_\infty = T_\infty - T_{sat} = \frac{\rho_l}{\rho_l - \rho_v}\frac{A}{R_c} \tag{13}$$

Eq. (6) can be expressed in dimensionless form in accordance with

$$\frac{\theta(y)}{\theta_\infty} = \frac{T(y) - T_{sat}}{T_\infty - T_{sat}} = \frac{T_w - T_{sat}}{T_\infty - T_{sat}}\left(1 - \frac{y}{\delta}\right) = \frac{\theta_w}{\theta_\infty}\left(1 - \frac{y}{\delta}\right) \tag{14}$$

and assuming that $\rho_l \gg \rho_v$, Eqs. (10) and (13) can be combined to give

$$\frac{\theta_w}{\theta_\infty}\left(1 - \frac{y}{\delta}\right) = \frac{R_c}{2}\left(\frac{1}{R_1} + \frac{1}{R_2}\right) \tag{15}$$

Finally, the equation to be solved in order to determine the profile of the vapour nucleus is

$$\frac{\theta_w}{\theta_\infty}\left(1 - \frac{y}{\delta}\right) = -\frac{R_c}{2}\frac{1}{r}\left[\frac{d}{dr}\left(\frac{ry'}{\sqrt{1+y'^2}}\right)\right] \tag{16}$$

$$\frac{\theta_w}{\theta_\infty}\left(1 - Y\left(\frac{R_c}{\delta}\right)\right) = -\frac{1}{2}\frac{1}{R}\left[\frac{d}{dR}\left(\frac{RY'}{\sqrt{1+Y'^2}}\right)\right] \tag{17}$$

in which $R = r/R_c$ is dimensionless radius and $Y = y/R_c$ is dimensionless displacement.

Using the assumption that $\beta = 90°$, the boundary conditions associated with Eq. (17) are $Y(1) = 0$, $Y'(1) = \tan\beta = \infty$ and $Y'(0) = 0$. Eq. (17) can then be solved in order to obtain the combinations of θ_w/θ_∞ and R_c/δ that satisfy it as well as the corresponding dimensionless vapour nucleus height $Y(0) = b/R_c$. The analytical solution to this problem is mathematically involved and Madejski presented it in a graphical form in which dimensionless wall superheat θ_w/θ_∞ and dimensionless vapour nucleus height b/R_c were plotted as a function of the dimensionless liquid temperature gradient R_c/δ.

The Madejski nucleation criterion curve, the locus of the values of θ_w/θ_∞ versus b/R_c determined by Eq. (17) for a number of values of R_c/δ, appears in the plot of θ/θ_∞ versus y/R_c which is presented in Fig. 2. Similar to Fig. 1, this figure schematically depicts the development of the dimensionless temperature profiles θ/θ_∞ in a liquid adjacent to a surface having superheat θ_w as a function of dimensionless distance $\delta/R_c = \sqrt{\pi\alpha_l t_w}/R_c$ where R_c is the radius of the hemispherical vapour nucleus. Initially, when the bulk liquid that replaces a departed bubble contacts the heated surface, the temperature gradient at the heated surface $d\theta(0,0)/dy = R_c/\delta = \infty$ so $b/R_c = 0$ and the vapour/liquid interface is planar. However, as time elapses and energy diffuses into the liquid, the temperature distributions $\theta(y,t)/\theta_\infty$ develop, the temperature gradient at the heated surface R_c/δ decreases and the height of the vapour nucleus b/R_c increases. Nucleation can occur whenever the temperature distribution curve intersects the Madejski nucleation criterion curve at the point corresponding to the dimensionless temperature gradient R_c/δ which implies that there is a net inward flow of heat even though the nucleus is spheroidal. As depicted in Fig. 2 for $\theta_w/\theta_\infty = 2.50$, nucleation occurs when the asymptote to the temperature profile in the liquid at the end of the waiting time t_w passes through the point on the Madejski nucleation criterion curve at which $\theta/\theta_\infty = 1.428$ and $b/R_c = 0.837$ in as much as the value of $R_c/\delta = 0.50$ corresponding to these values according to the solution of Eq. (17) is the same as that of the asymptote to the temperature distribution curve at time $t = t_w$ for which $\delta/R_c = 2.00$.

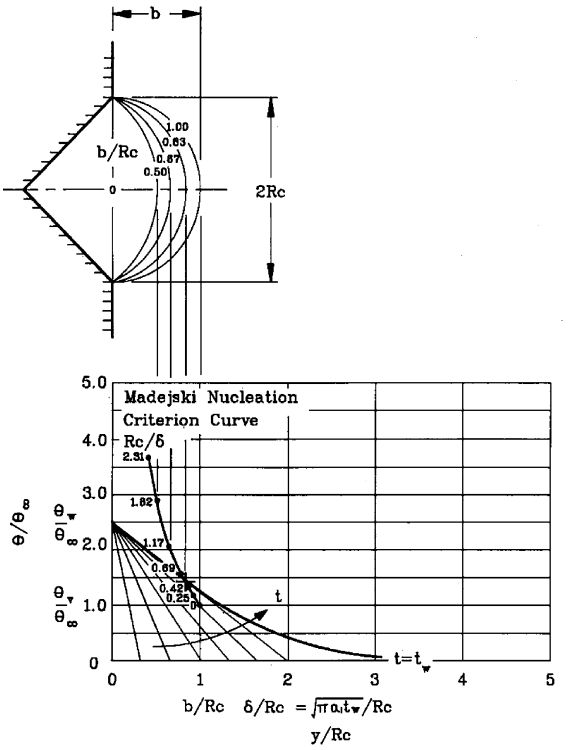

Fig. 2. Schematic representation of the Madejski nucleation theory.

4. Experimental set-up and procedure

The experimental apparatus employed was able to maintain and closely control the boiling conditions, such

as heat flux, temperature of the liquid in the boiling vessel and system pressure, so that the locations of each nucleation site on the heater surface could be identified and the time elapsed between the appearances of bubbles at the nucleation sites after the power had been switched on could be determined. A detailed description of the apparatus with all its components and associated equipment follows.

The soda-lime glass panels used in the investigation were supplied by Hartford Glass Inc., Indiana. The surface of the panels were coated with a 300 nm ± 10% thick electro-conductive tin oxide film with a total electrical resistance of approximately 26 Ω. Silver contact bands, which had almost zero resistance, facilitated uniform generation of heat when an electric current was applied. The heat flux $q'' = q/A$ was easily adjusted by independently setting the current I and/or the voltage E at the desired levels.

A cross sectional view of the boiling vessel which was 240 mm high by 150 mm in diameter is shown in Fig. 3. The sight tube was used to monitor the level of the liquid and to observe the boiling activity at the heater surface. A condenser coil was installed below the top plate to condense the vapours generated in order to facilitate the establishment of equilibrium conditions in the boiling vessel. The system pressure was maintained by a vacuum pump which drew vapour from the boiling vessel through a reflux condenser at the top of the vessel to minimize vapours being drawn into it.

The heater surface was located over the opening in the base plate of the boiling vessel through which the observations were made. A Teflon ring gasket sealed the base and the cover plate to the vessel wall and the whole apparatus was connected with eight tie-down bolts. Power was supplied through bus bars to the clamps that were isolated from the base by Teflon shims. For maximum flexibility, the contact between the clamp and the silver contact band on the glass was made by means of 1 cm wide strips of aluminum foil wrapped around cylindrical pieces of Viton rubber. A Viton O-ring was used to seal the glass panel in the recess in the base plate that contained it. The aluminum clamp that compressed the O-ring was fastened to the base plate by machine screws and chamfered at a 45° angle to distribute the pressure force uniformly between the glass panel and the base plate. The seal created in this way was able to sustain up to one half-atmosphere vacuum.

The images of the bubbles forming on the upper surface of the glass panel were captured by means of a Kodak EktaPro high-speed video camera capable of recording images up to 1000 frames per second. Illumination for the camera was provided by a Spectra-Physics 125 A helium–neon gas laser with a Model 261 RF/DC Exciter. The monochromatic laser beam emitted had a wave length of 632.8 nm and was 2 mm in diameter. After being expanded to approximately 20 mm diameter by a convex lens and collimator, it was directed toward the glass heater surface by the mirror shown in Fig. 4.

The footprint of a growing bubble reflects more light than the bubble due to the higher coefficient of refraction of the vapour phase as compared to the liquid phase. The reflected image was directed to the high-speed video camera by a semi-transparent prism. Al-

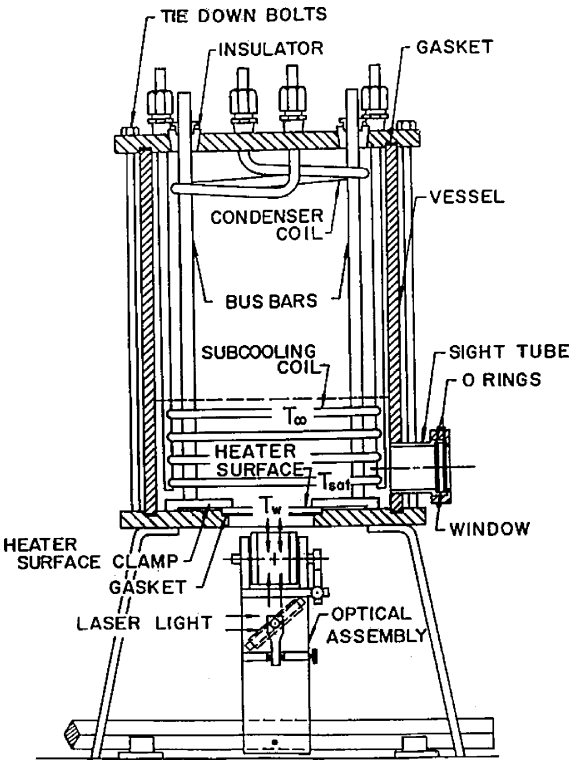

Fig. 3. Cross sectional view of the boiling vessel.

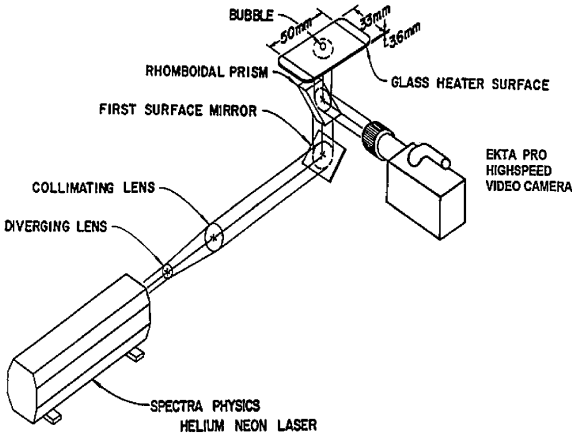

Fig. 4. Schematic representation of the optical assembly.

though the footprint of a bubble is much smaller than the bubble itself, the magnification of the optical system, which was approximately 25 times, enabled observation of bubbles as small as 0.5 mm. Focused images of the flashes created by the bubbles appearing on the glass heater surface were obtained through two lenses, a Soligor Tele Auto 1:2.8 $f = 105$ mm and a Pentax Macro-Tacumar 1:4/50. The image captured was processed by the Kodak EktaPro Processor and displayed on a Sony Trinitron monitor.

Dichloromethane (methylene chloride), the boiling fluid used in the investigation, is a clear, colourless, volatile organic liquid, with a sweet odour which is slightly irritating to the eyes. Its principal use has been as a solvent, aerosol propellant and decreasing agent. Dichloromethane was chosen for this investigation because it has a relatively low boiling point of 39 °C at atmospheric pressure and because an organic liquid was required for compatibility with the stannic oxide coating on the glass panel.

The Kepco power supply (model JQE 150-3.5M) used could provide up to 150 V or 3.5 A and offered the capability of independently setting the limits of either the current or the voltage. Although the power supply was equipped with an ammeter and voltmeter, digital multimeters were employed for increased accuracy, producing errors of only ±0.2 V or about 0.4% of the full scale voltage reading, and ±0.05 A or approximately 2% of the full scale current reading.

For the experiments performed below atmospheric pressure, vacuum was created by a Duo Seal vacuum pump made by the W.M. Welch Manufacturing Co., connected to the boiling vessel through the reflux condenser. While the vacuum pump ran at constant (maximum) flow rate, the desired pressure was obtained by regulating an adjustable bleed valve located on the top of the apparatus which was open to the atmosphere and reading a mercury manometer. By constantly adjusting the bleed valve, pressure variations were reduced to ±0.2 in. Hg or about 650 Pa.

Upon applying a step change in heat flux by turning the power supply on, the camera was triggered by a power supply/camera interface, designed and constructed by the electronics specialist in the Department of Mechanical Engineering. The interface introduced a time delay of approximately 1.4 ms in the measurements of elapsed time associated with the initial response, which was deemed to be insignificant.

Chromel–Constantan (Type E) thermocouples were used throughout the investigation. One thermocouple was attached to the glass panel to measure the heater surface temperature and another one was placed a few millimeters above the heater surface to monitor the liquid temperature. The thermocouple leads were connected through an ice bath to an Escort 97 multidisplay multimeter reading up to 0.001 mV, introducing uncertainty of approximately ±0.01 mV or 0.2 °C. The readings were found to be in good ±0.5 °C agreement with a mercury type thermometer at room temperature and at the boiling temperature of the dichloromethane.

The glass panels as received from the supplier were quite smooth and contained virtually no or extremely few nucleation cavities. In this form, the glass panels would start producing bubbles when the superheat exceeded 35 °C, under which conditions the panels were prone to breaking. One way to improve the performance of the surface was to patiently age it. Aging is a naturally occurring process of breaking in the surface and developing surface imperfections and potential nucleation sites. By carefully increasing the power and thus the glass temperature, it is possible to age the glass sufficiently over a period of time. However, this process would often take more than a couple of weeks of nonstop boiling during which period the glass might break due to fatigue.

The final step of the preparation was to determine the locations of the nucleation sites existing on the heater surface. After turning the power off and on again shortly afterward, boiling would resume at the most active nucleation sites. Twenty sites spaced sufficiently far apart from one another to avoid interaction were deemed to be suitable for examination so that the experiments could commence.

5. Experimental results

Experimental results were obtained at 15 different nucleation sites. For each nucleation site, different combinations of heat flux and system pressure were investigated. Depending on the consistency of the values obtained, 5–20 repeat tests were performed. The results reported are averages of the values obtained.

After boiling had occurred for more than half an hour at a particular heat flux and steady state had been established, the power would be turned off. The heat contained in the heater surface would diffuse into the liquid and the wall temperature T_w would approach the saturation temperature of the liquid T_{sat} at that system pressure. Upon restoration of power, representing a step change in heat flux q'', boiling would resume.

The high-speed video camera recorded the appearance of the initial and subsequent bubbles at each nucleation site investigated. From slow-motion replay, the time elapsed until the formation of the initial bubble $\tau_{initial}$ and the time elapsed between the formations of the subsequent bubbles $\tau_{subsequent}$ was determined. The results presented in Fig. 5, obtained for site IX at which only two bubbles nucleated after the initial bubble, are deemed to be a good representation of the elapsed times measured throughout the course of the investigation. Sites at which more subsequent bubbles nucleated

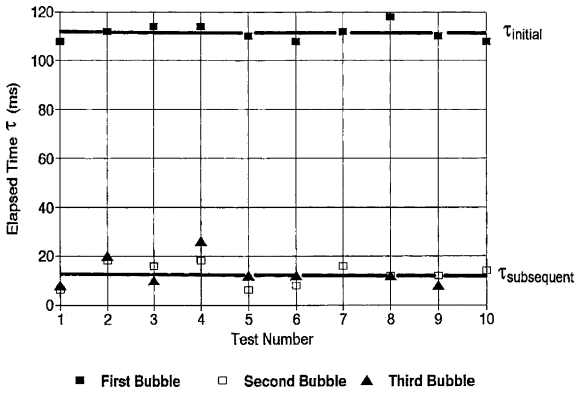

Fig. 5. Bubble formation periods at site IX for $q'' = 109.6$ kW/m^2 and $p_{sat} = 99.4$ kPa.

showed the same trend in as much as there was great consistency among the measurements of elapsed time for the subsequent bubbles. It would seem that the physical phenomenon governing the appearance of the initial bubble is different from the physical phenomenon governing the appearance of the subsequent bubbles.

6. Analysis and discussion

6.1. Determination of growth and waiting times

The elapsed time intervals between the appearance of two consecutive bubbles forming at the same nucleation site on the heater surface τ is comprised of waiting and growth time periods in accordance with $\tau = t_g + t_w$. The waiting and growth times periods were not measured independently, but the values that are needed for the subsequent analysis can be determined from a unique relationship that arises from the bubble growth theory developed by Rohsenow and coworkers [8,9]. This theory has been applied successfully in a number of boiling heat transfer investigations and found to be in good agreement with the experimental results [10,11].

According to Rohsenow and coworkers, the radius of a bubble at all stages of growth in saturated boiling liquid can be predicted by the relationship

$$R(t) = 2\sqrt{\frac{3}{\pi}} Ja \sqrt{\alpha_l}\left(\sqrt{t} - \sqrt{t + t_w} + \sqrt{t_w}\right) \tag{18}$$

According to Cole [12], the bubble departure radius at the end of period τ is given by

$$\overline{R}_b = 0.016\sqrt{\frac{\sigma}{g(\rho_l - \rho_v)}} Ja \tag{19}$$

Setting $R(t_g) = \overline{R}_b$ and using the properties of dichloromethane evaluated at $T_{sat} = 39$ °C to evaluate the parameter grouping $0.016\sqrt{\sigma/g(\rho_l - \rho_v)}/2\sqrt{3/\pi}\sqrt{\alpha_l} = 1.229$ yields

$$\left(\sqrt{t_g} - \sqrt{t_g + t_w} + \sqrt{t_w}\right) = 1.229 \tag{20}$$

where t_g and t_w are expressed in milliseconds. This equation can be solved simultaneously with $\tau = t_g + t_w$ to obtain the values of t_w and t_g corresponding to all bubble periods τ.

As seen in Fig. 5, the initial bubble elapsed times differed considerably from the subsequent bubble elapsed times. When electric power is applied, the heat generated in the coating on the glass panel diffuses simultaneously into the heater surface and the adjacent liquid, according to the relationship $q'' = q''_s + q''_l$. Treating the bodies as semi-infinite solid domains subjected to constant heat flux, the Fourier equation can be solved to determine the transient temperature distributions subject to the boundary conditions $\theta_l(y,0) = 0$, $\theta_l(\infty,t) = 0$, $\partial\theta_l(0,t)/\partial y = -q''_l/k_l$ and $\theta_s(-y,0) = 0$, $\theta_s(-\infty,t) = 0$, $\partial\theta_s(0,t)/\partial y = -q''_s/k_s$ leading to

$$\begin{aligned}\theta(y,t) &= \frac{q''_l}{k_l} 2\sqrt{\alpha_l t}\,\mathrm{ierfc}\left(\frac{y}{2\sqrt{\alpha_l t}}\right) \\ &= \frac{q''_s}{k_s} 2\sqrt{\alpha_s t}\,\mathrm{ierfc}\left(\frac{-y}{2\sqrt{\alpha_s t}}\right)\end{aligned} \tag{21}$$

The transient temperature distributions in the solid and the liquid leading up to the moment at which the first bubble commences to develop are depicted in Fig. 6. After the power has been turned on, the temperature of the heater surface rises until it attains the steady state superheat θ_{sup} in time interval $\tau_{initial}$ at which time the first bubble nucleates. It can be seen that roughly three quarters of the heat generated diffuses into the solid while roughly one quarter of the heat diffuses into the liquid. Once the heater surface has attained steady state conditions, the superheat remains invariant in as much

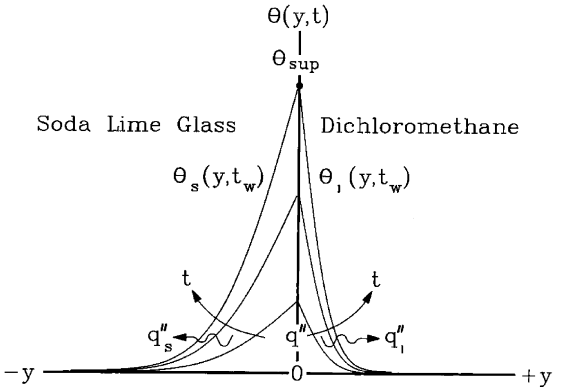

Fig. 6. Temperature profiles in adjacent semi-infinite domains representing the surface and the liquid subjected to a constant heat flux at the interface.

as the formation and departure of the subsequent bubbles at time intervals $\tau_{subsequent}$ is able to remove the heat at the rate that it is generated.

6.2. Evaluation of the classical nucleation theory

Classical nucleation theory is based upon the assumption that a hemispherical nucleus having the same radius R_c as the nucleation cavity at which it is located appears after the departure of the previous bubble and awaits the conditions required to nucleate a bubble. As explained before, this will occur when the temperature of the liquid surrounding the nucleus is sufficiently greater than the temperature of the vapour in the nucleus that there is a net flow of heat inward, thereby enabling the nucleus to grow. This condition is ensured if the liquid temperature distribution passes through the point corresponding to the tip of the nucleus where $y = b$ and $\theta = \theta_v$. It follows, therefore, that the liquid temperature distribution at the end of the waiting period t_w when the nucleus commences to develop into a bubble must always pass through the same point on a plot of temperature difference θ/θ_∞ versus distance perpendicular to the heater surface y/R_c no matter what the value of the impressed heat flux q''.

Fig. 7 is a plot of the asymptotes to the dimensionless temperature profiles θ/θ_∞ versus $y/\sqrt{\pi\alpha_l t_w}$ that existed at the moment at which the nucleus at site IX began to develop into a bubble for the four different levels of heat flux at which investigations were conducted at a system pressure $p_{sat} = 99.4$ kPa. The figure is conceptually identical to Fig. 1 except that the intermediate asymptotes corresponding to values of time between $t = 0$ and $t = t_w$ have been omitted for the sake of clarity. Although the lines appear to intersect, the intersection does not occur at the point representing the Classical nucleation criterion at which $\theta_v/\theta_\infty = 1$ and $b/R_c = 1$.

More particularly, the Classical nucleation criterion expressed by Eq. (5) is not satisfied. There is no single value of cavity radius R_c which will satisfy the equation for all of the different levels of heat flux at which investigations were conducted as there ought to be in as much as the experimental results presented in Fig. 7 were all obtained at the same nucleation site. A single value of nucleation cavity radius $R_c = 0.525$ μm that fit the results best was used to plot the straight lines in Fig. 7 but it can be seen that the straight lines resulting from this choice of nucleation cavity radius intersect to the right and below the point representing the Classical nucleation theory. As a consequence, it may be concluded that the experimental results do not support the Classical nucleation criterion. The same conclusion was found with respect to all of the other investigations conducted at different nucleation sites for various levels of heat flux and system pressure.

6.3. Analysis of the Madejski nucleation theory

Because of the complexity involved, it is not practical to demonstrate the Madejski nucleation criterion in the same way as the Classical nucleation criterion by plotting the results on a graph. Instead, the validity of the theory was tested by using it to determine the radius of the cavity at which nucleation had occurred, which obviously should be a unique value for a particular nucleation site, under different conditions and observing

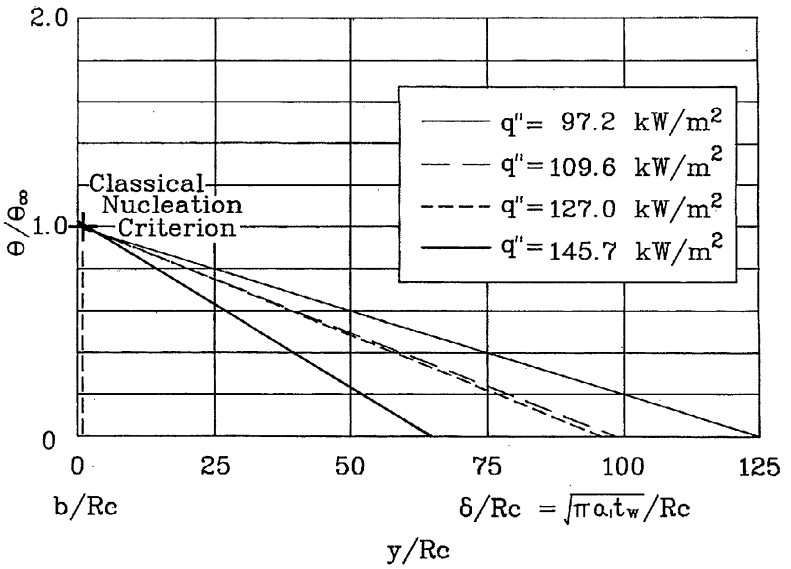

Fig. 7. Analysis of bubble formation at site IX using the Classical nucleation theory.

Table 1
Analysis of the experimental results for site IX at $p_{sat} = 99.4$ kPa

q'' (kW/m^2)	θ_w (°C)	τ (ms)	t_g (ms)	t_w (ms)	δ (μm)	θ_∞ (°C)	θ_w/θ_∞ (–)	δ/R_c (–)	R_c (μm)
97.2	27.9	18.9	2.231	16.669	66.14	27.5	1.0160	123.72	0.5346
109.6	28.1	12.8	2.603	10.197	51.73	27.6	1.0199	97.09	0.5328
127.0	28.3	12.3	2.662	9.638	50.29	27.6	1.0289	96.39	0.5337
145.7	28.7	8.4	4.000	4.400	33.98	28.2	1.0199	63.67	0.5217

Table 2
Analysis of the experimental results for site IX at $p_{sat} = 62.2$ kPa

q'' (kW/m^2)	θ_w (°C)	τ (ms)	t_g (ms)	t_w (ms)	δ (μm)	θ_∞ (°C)	θ_w/θ_∞ (–)	δ/R_c (–)	R_c (μm)
108.7	27.4	18.7	2.238	16.462	65.73	27.0	1.0165	120.69	0.5446
126.1	27.9	14.9	2.424	12.476	57.22	27.5	1.0183	106.79	0.5358
144.6	28.3	13.8	2.507	11.293	54.44	27.9	1.0188	103.01	0.5285

the consistency of the values obtained. Tables 1 and 2 present the analysis of the results obtained for the investigations performed at nucleation site IX at a number of different levels of heat flux and two levels of system pressure.

It is evident that the values of cavity radius obtained for nucleation site IX at different levels of heat flux and system pressure are essentially the same. The individual values of cavity radius obtained are very consistent differing from one to another by only a few percent, thereby attesting to the validity of the theory.

Fig. 8 presents similar results for nine of the nucleation sites to which the Madejski nucleation criterion had been applied. Although the values of nucleation cavity radius vary from cavity to cavity, as might be expected, the values obtained for a particular cavity are virtually independent of heat flux and system pressure. The excellence of the agreement supports the the Madejski nucleation criterion but further research in which the effective radius of the nucleation cavity can be shown to correspond to the value inferred by the analysis described above is required before it can be claimed that the Madejski nucleation criterion has been validated.

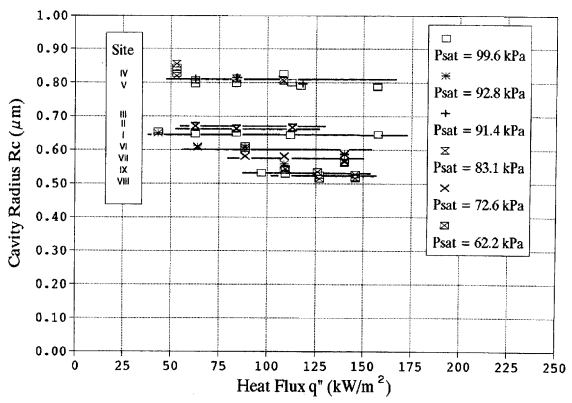

Fig. 8. Analysis of bubble formation at nine sites using the Madejski nucleation theory.

7. Conclusion

Based upon an analysis of the formation of bubbles in response to a step change in heat flux at different levels of heat flux and system pressure, it was determined that the Classical nucleation criterion was not able to predict the conditions required for a bubble to nucleate. The Madejski nucleation criterion appeared to be in good agreement with the observations, however, in as much as most of the values of cavity radius obtained at each of the different nucleation sites by applying the Madejski nucleation criterion were consistently within one percent of each other at all levels of heat flux and system pressure. While it is undeniable that every nucleus must pass through the hemispherical shape before a bubble begins to develop, it seems that nucleation does not depend upon the development of a superheated liquid layer thick enough to completely immerse a hemispherical nucleus as required by the Classical nucleation criterion. The Madejski nucleation criterion requires only a net flow of heat into the nucleus, which will be spheroidal in shape depending upon the temperature gradient existing in the liquid at the moment that the condition is satisfied, after which the nucleus will quickly achieve the hemispherical shape and bubble nucleation will occur immediately thereafter.

References

[1] J.W. Westwater, Boiling heat transfer, Am. Scientist 47 (1959) 427–446.
[2] S.G. Bankoff, Entrapment of gas in the spreading of a liquid over a rough surface, AIChE J. 4 (1958) 24–26.

[3] Y.Y. Hsu, On the size range of active nucleation cavities on a heating surface, J. Heat Transfer 84 (1962) 204–216.
[4] C. Han, P. Griffith, The mechanism of heat transfer in nucleate pool boiling, Int. J. Heat Mass Transfer 8 (1965) 887–904.
[5] M. Shoukri, R.L. Judd, Nucleation site activation in saturated boiling, J. Heat Transfer 97 (1975) 93–98.
[6] J.R. Howell, R. Siegel, Incipience, growth and detachment of boiling bubbles in saturated water from artificial nucleation sites of known geometry and size, paper 114, in: Proceedings of the Third International Heat Transfer Conference, 1966, pp. 12–23.
[7] J. Madejski, Activation of nucleation cavities on a heating surface with temperature gradient in a superheated liquid, Int. J. Heat Mass Transfer 9 (1966) 295–300.
[8] B.B. Mikic, W.M. Rohsenow, Bubble growth rates in non-uniform temperature field, Progr. Heat Mass Transfer (1969) 283–293.
[9] B.B. Mikic, W.M. Rohsenow, P. Griffith, On bubble growth rates, Int. J. Heat Mass Transfer 13 (1970) 657–665.
[10] E.A. Ibrahim, R.L. Judd, An experimental investigation of the effect of subcooling on bubble growth and waiting time in nucleate boiling, ASME J. Heat Transfer 107 (1985) 168–174.
[11] R.L. Judd, The role of bubble waiting time in steady nucleate boiling, ASME J. Heat Transfer 121 (1999) 852–855.
[12] R. Cole, Bubble frequencies and departure volumes as subatmospheric pressures, AIChE J. 13 (1967) 779–783.